Buckling and Failure of Sandwich Plates with Graphite-Epoxy Faces and Various Cores

Pierre Minguet,* John Dugundji,† and Paul A. Lagace‡
Massachusetts Institute of Technology, Cambridge, Massachusetts

A study of the compressive failure of sandwich plates was conducted. Twenty-one panels (250 × 250 mm) were manufactured with $[+45/-45/0]_s$ graphite-epoxy face sheets and three types of cores – Nomex honeycomb, Rohacell foam, and aluminum honeycomb – in three different thicknesses – 3.2, 6.4, and 9.6 mm. These panels were tested under uniaxial compression with clamped loaded edges and simply supported sides, and overall buckling was the only type of instability that was observed here. The effects of these different cores were investigated, and three types of failure modes were observed – core failure, disbond, and face fracture. Initial out-of-plane imperfections were found to have an important effect on the final failure load for thick panels but only a small influence for thin panels. Using the stresses predicted by a nonlinear analysis and appropriate failure criteria, namely maximum transverse shear stress for the core or bond failure and stress interaction for the face fracture, failure load predictions that are in good agreement with the experimental data can be made.

Introduction

SANDWICH construction has been used in aeronautical applications for more than 40 years, since it offers the possibility of achieving a high bending stiffness for a small weight penalty. Today, there is renewed interest in using sandwich structures and several recent airplanes, such as the Beech Starship and the Voyager, are making extensive use of this type of construction for primary structural components. The main reason for this increase in use of sandwich panels is the introduction of new materials such as composite materials for the faces, which offer a long-awaited capability with both high stiffness and low specific weight. Similarly, new materials for the core are now available, such as nonmetallic honeycombs and plastic foams. Since composite materials do not exhibit large yelding deformation prior to failure as metals do and thus do not allow as much error or approximation in their design, new experimental data are needed to assess their usefulness, and better analysis techniques must be developed to help predict their behavior.

Compressive loadings are inevitable in most aerospace structures, and buckling of panels is therefore of prime concern. One classical way of preventing this has been to use stiffeners of various shapes to reinforce the structure's skin. Sandwich panels offer an interesting alternative to this since they can achieve a similar bending stiffness, and therefore buckling load, without the manufacturing complexity of a stiffened structure and the joints between different components. The use of sandwich structure does introduce the possibility of various failure modes under compression, which can be generally grouped into two categories: instabilities, such as overall buckling and face wrinkling caused by insufficient plate or face bending stiffness and core elastic properties,[1-3] and fracture, either of the face sheets under compression or of the core under transverse shear stresses.[4]

Extensive testing of various sandwich configurations has been done at the U.S. Forest Product Laboratory for more than 40 years.[5] Recent references regarding the use of advanced composite face sheets are unfortunately scarcer (in the open literature), and some can be found in a recent survey by Leissa.[6] A good example of an experimental study of buckling and wrinkling can be found in Ref. 7, where Pearce and Webber tested a few sandwich panels with graphite-epoxy faces. However, more work remains to be accomplished. In this paper, the main results of a recent study on the compressive failure of sandwich structures are presented. More detailed experimental and analytical results from this study can be found in Ref. 8.

Received March 31, 1987; presented as Paper 87-0795 at the 28th AIAA/ASME/ASCE/AHS Structures, Structural Dynamics and Materials Conference, Monterey, CA, April 6-8, 1987; revision received Aug. 15, 1987.

*Research Assistant, Technology Laboratory for Advanced Composites, Department of Aeronautics and Astronautics.
†Professor, Department of Aeronautics and Astronautics. Member AIAA.
‡Associate Professor, Department of Aeronautics and Astronautics. Member AIAA.

Experiment

Program Layout

The two variables of interest in the experiment are the core thickness and the core material properties. To allow for proper comparison of the results in terms of core properties, three different core materials were chosen with approximately the same density of 80 kg/m^3: aluminum honeycomb, Nomex honeycomb (made from aramid paper impregnated with phenolic resin), and Rohacell foam (a closed-cell rigid polymethacrylic imide expanded plastic). Their material properties are indicated in Table 1. Although the Rohacell foam has a fairly low shear stiffness, it could have some advantages over the Nomex honeycomb, such as the possibility of being thermoformed to achieve curved surfaces. Three different thicknesses – 3.2, 6.4, and 9.6 mm – were used for the Nomex and Rohacell. The aluminum honeycomb was intended to be a baseline comparison and, therefore, only the 6.4-mm thickness was utilized.

Hercules AS4/3501-6 graphite-epoxy was used for the face sheets, and material properties for this material are also listed in Table 1. After some preliminary buckling load estimates, a $[+45/-45/0]_s$ layup was adopted for each face sheet to limit the loads involved for the capacity of the testing machine. The ± 45 deg plies provide the necessary transverse bending stiffness and are placed on the outside to avoid any possibility of the 0 deg plies buckling away prematurely.[9] Also, no matrix cracking occurs in this laminate up to failure as it might in laminates with 90 deg plies. The same type of boundary conditions were used for all the specimens, namely clamped loaded edges and simply supported sides.

A minimum of three samples of each type were tested to obtain meaningful results, which gave a total of 21 panels for the test matrix shown in Table 2. The notation *XI-J* was used to identify the different plates, where *X* identifies the core type and can take the value A for Aluminum honeycomb, N for Nomex honeycomb, or R for Rohacell foam. *I* represents the thickness and takes the value 1 for a 3.2-mm core thickness, 2 for a 6.4-mm core thickness, or 3 for a 9.6-mm core thickness, and *J* represents the specimen number of that particular type. Thus, for instance, N2-3 represents the Nomex core, 6.2 mm thick, third specimen.

Table 1 Panel material properties

AS4/3501-6 face sheets:

E_L:	139.3 GPa	X_T:	2150 MPa
E_T:	11.1 GPa	X_C:	1550 MPa
G_{LT}:	6.0 GPa	Y_T:	54 MPa
ν_{LT}:	0.3 GPa	Y_C:	221 MPa
		S:	105 MPa

Ply thickness: 0.134 mm
Each face sheet is $[+45/-45/0]_s$

Core materials (MPa)

Material	Transverse moduli G_{xz}	G_{yz}	Strength τ_{xz}	τ_{yz}
Aluminum honeycomb	390	190	1.7	1.1
Nomex honeycomb	60	30	1.8	1.2
Rohacell foam	34	34	1.3	1.3

Table 2 Test matrix

Core type	Core thickness, mm 3.2	6.4	9.6
Aluminum honeycomb	–	3[a] (A2)[b]	—
Nomex honeycomb	3 (N1)	3 (N2)	3 (N3)
Rohacell foam	3 (R1)	3 (R2)	3 (R3)

All face sheets are $[+45/-45/0]_s$ graphite-epoxy. [a]Number indicates number os specimens tested. [b]Shortened for core type and thickness.

Manufacture

Standard procedures were used for all manufacturing of the panels, which took place in a two-part operation.[10] The first part involved the preparation of 320 × 290 mm $[+45/-45/0]_s$ graphite-epoxy face sheets. These were cured in an autoclave under 0.54 MPa pressure and 760 mm Hg vacuum with a 1 h hold at 116°C and a 2 h hold at 177°C. After an 8 h postcure at 177°C, the laminate edges were trimmed off on a milling machine equipped with a diamond-grit wheel and water cooling.

The second part involved core preparation and secondary bonding. The core materials were cut and swept clean of any particles and fibers. The aluminum honeycomb was additionally cleaned by soaking for 5 min in methylethylketone. The graphite-epoxy face sheets were also cleaned with alcohol. Sheets of American Cyanamid FM123-2 modified nitrile-epoxy film adhesive were prepared in the same size as the core material pieces, and the sandwich panels were assembled. The bonding cure cycle consisted of 2 h at 107°C under 0.28 MPa external pressure. No vacuum was applied to the sandwich plates in an effort to avoid collapsing the honeycomb cells, and the vacuum bag was vented to atmosphere.

These test specimens were then cut to their final size. The most important requirement here was to assure that the loaded edges of the panels were parallel in order to obtain uniform loading during testing. The cutting was done on the same milling machine previously mentioned, resulting in a panel size of 292 mm in length by 273 mm in width with a tolerance of 1 mm. A jig was used to hold the panels during this operation so that the average difference in length along the sides was less than 0.2 mm, which is less than 0.1% of the total specimen length.

Two pairs of back-to-back strain gages were then mounted on each plate, located on the horizontal center line, 25 mm on the right and left of the center, oriented along the loading direction. This resulted in the final specimen configuration, shown in Fig. 1. Back-to-back strain gages were necessary to separate the membrane and bending components of the strains. Differences in readings from strain gages placed on the same face can also be used to estimate how uniformly the load is introduced.

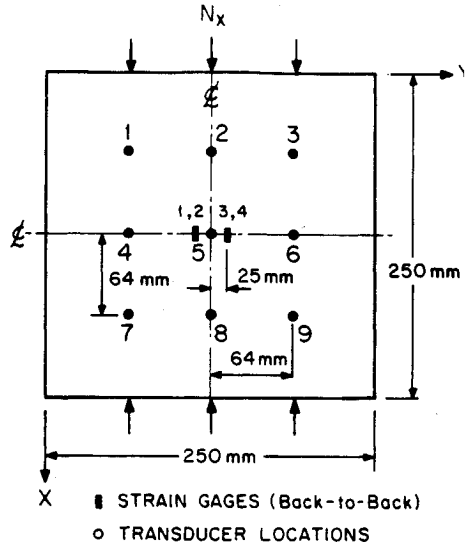

Fig. 1 Test specimen configuration.

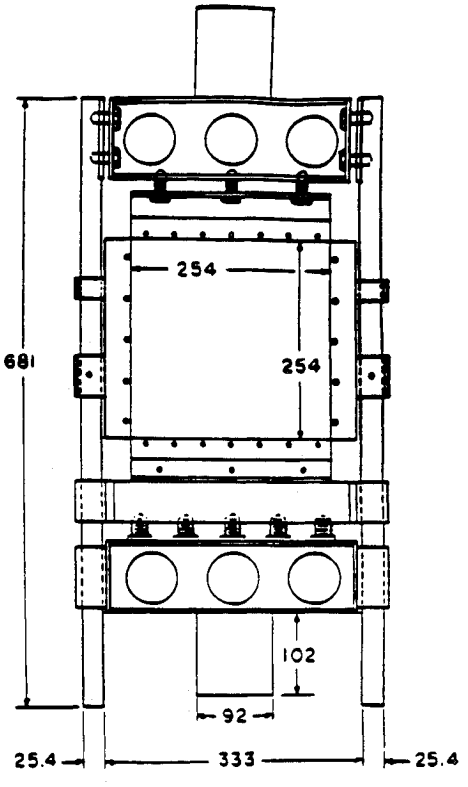

Fig. 2 Sketch of buckling jig.

Testing Setup

Testing was accomplished using a buckling test fixture mounted in the hydraulic grips of a 445-kN (100,000-lb) MTS 810 testing machine. This buckling jig, illustrated in Fig. 2, was similar to the one used in Ref. 11, and its detailed description can be found there. The specimens are loaded directly by contact, since sufficient care had been taken in maching the plates to insure that the edges are parallel. However, during the testing of the first plate with a 9.6 mm Nomex core, another type of problem was encountered. At a load of about 130 kN, the loaded edges buckled inside the fixture, crushed the core, and collapsed. In order to avoid this, the two other plates of that type had their edges potted in aluminum channels with an epoxy resin. This procedure may be necessary for tests conducted at these higher loads. At the

lower loads encountered by all the other types of plates, loading the specimen by contact was satisfactory.

Simply supported side boundary conditions were used for all tests. These consisted of two pairs of rounded knife edges held against the plate by several bolts. To minimize the introduction of extraneous loads due to friction along the supports, the vertical edges of the specimens were covered with a layer of Teflon tape and lubricated with a molybdenum-lithium compound.

In addition to the strain gage data mentioned previously, in-plane and out-of-plane displacement data were taken during the tests. The end-shortening of the plate was recorded by a linear variable differential transformer (LVDT) mounted vertically alongside the jig. The lateral deflections w were measured at nine locations by transducers mounted on a back rack. These were located in a 3 × 3 array, with a spacing of 64 mm in the horizontal and vertical directions from the center of the panel as illustrated in Fig. 1. Testing was conducted in stroke control mode at a rate of 0.4 mm/min. During the whole test, data was automatically recorded at intervals of 0.5 s by a PDP 11/34 computer. Every plate was tested monotonically to failure, which was identified by a sudden drop in load carrying capability, usually of more that 90%.

Results

General Features

To illustrate the data obtained in these tests, the load deflection and load strain behaviors for a plate with a 3.2-mm Rohacell foam core are shown in Figs. 3 and 4. Because of the presence of initial out-of-plane deflections in the panel, transverse displacements develop from the onset of loading and grow relatively linearly until the buckling load is approached. Then, deflections rapidly increase and failure occurs relatively soon after. Also, for convenience, the experimental buckling load was defined as the load at which the strain reaches a maximum and starts decreasing on one face of the panel.

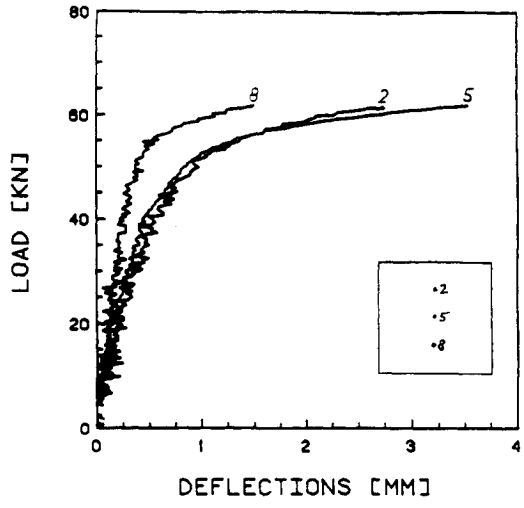

Fig. 3 Load deflection behavior for 3.2-mm Rohacell core panel.

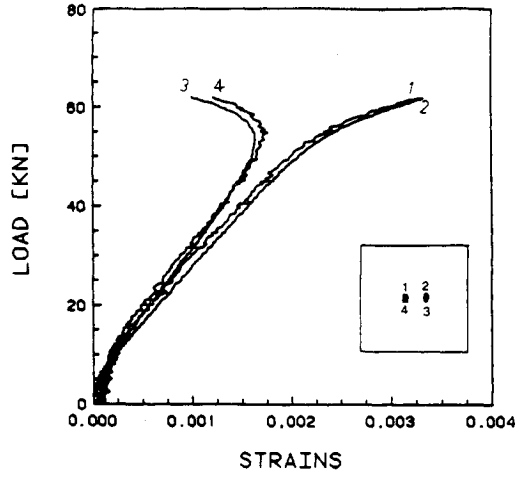

Fig. 4 Load strain behavior for 3.2-mm Rohcell core panel.

Table 3 Failure modes summary

Core	Aluminum	Nomex	Rohacell
3.2 mm	–	Bond	Core
6.4 mm	Face	Bond/face	Core
9.6 mm	–	Face	Core/faces

The failure loads of all the specimens tested are summarized graphically in Fig. 5 for each family of plates. All the panels tested exhibited an overall buckling type of behavior, and no evidence of face wrinkling was found for the range of thicknesses and properties that were tested. However, for the thickest plates, the shape of the buckling mode was slightly different from the shape for the thin plates, as illustrated in Fig. 6. For the 3.2-mm Rohacell foam core plate, the deformed shape is symmetrical with respect to the panel center, while for the 9.6-mm foam core, the deformed shape is a superposition of a first and second mode, resulting in maximum deflection not at the panel center. The same effect was observed for the Nomex core plates when the thickness was increased.

Three types of final failure modes were observed in the tests: core fracture, disbond at the interface between the film adhesive and the face sheets, and face fracture. Table 3 summarizes the different modes of failure observed for each type of plate. Face failure, which was the dominant mode for the plates with a 6.4-mm aluminum or 9.6-mm Nomex core, always occurred near one of the clamped edges, either all the way across the width of the plate or along a 45-deg line. The maximum strain reading (at the center of the panel) for these two types of plates was about 7000 microstrain. Bond failure occurred for all the plates with a 3.2-mm or 6.4-mm Nomex core and happened always in a wide band (50–100 mm), all across the width of the panel, located about halfway between the center of the plate and one of the loaded edges. Postfailure inspection of the disbonded area showed that virtually no graphite-epoxy was left bonded on the film adhesive. Core fracture, which happened in all the Rohacell foam core panels, was also always located halfway between the center of the panel and one of the clamped edges.

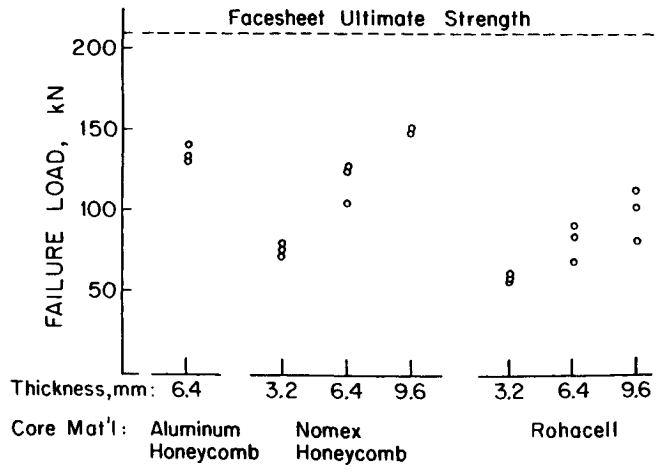

Fig. 5 Summary of experimental failure loads.

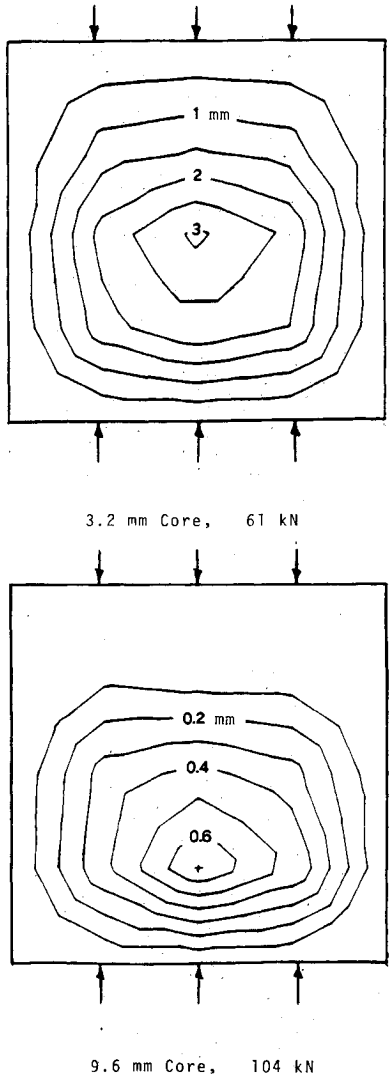

Fig. 6 Deflection contours for two different Rohacell panels near failure.

Core Thickness Effect

For a plate with a given core material and a given set of faces, increasing the core thickness changes the type of failure mode. Thinner panels will buckle at lower loads and will be able to go further into the postbuckling range; they then develop large deflections that cause transverse shear stresses in the core and at the bondline, which lead to the final failure while face damage remains small. Thicker panels, however, buckle at higher load, and the bending stresses that develop then add more to the membrane stresses compared to thinner panels, thus tending to cause larger face damage or even fracture.

Another consequence of an increased core thickness is an increased sensitivity to initial out-of-plane imperfections. This can be seen for instance in Fig. 5, especially for the Rohacell foam core family: one of the 9.6-mm core plates has a lower failure stress than a 6.4-mm one because of the presence of a large initial imperfection, as indicated by the slope of the load-deflection curve in the prebuckling region. As both experimental and later analytical results indicate, identical plates with different initial imperfections have different load-deflection behavior below their buckling load but tend to have similar deformations in the postbuckling region. Since the stresses caused by out-of-plane deflections are the main cause of failure, this tends to explain why thin panels, which fail well above their buckling load, are less sensitive to these imperfections than thick plates, which fail below their buckling load.

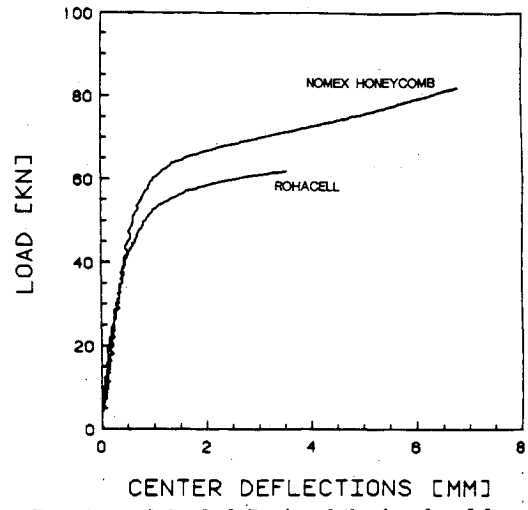

Fig. 7 Experimental load deflection behavior for 3.2-mm core panels.

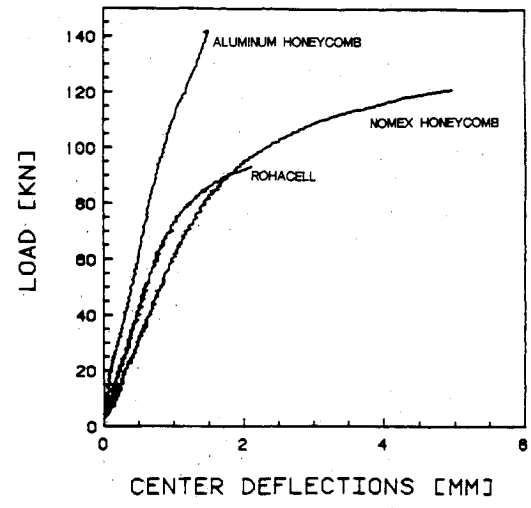

Fig. 8 Experimental load deflection behavior for 6.4-mm core panels.

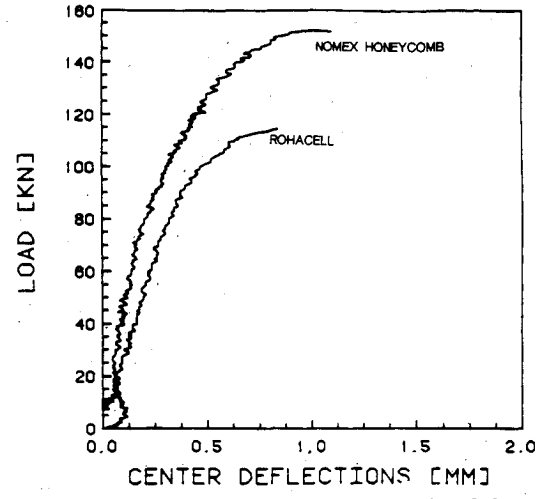

Fig. 9 Experimental load deflection behavior for 9.6-mm core panels.

Core Material Effect

The major core material properties of interest in this problem are the shear modulus and ultimate strength. The higher these are, the better the sandwich panel will perform under axial compressive load, disregarding other properties like heat, moisture and fatigue resistance, formability, cost, etc., which were not considered here. Figures 7–9 show typical

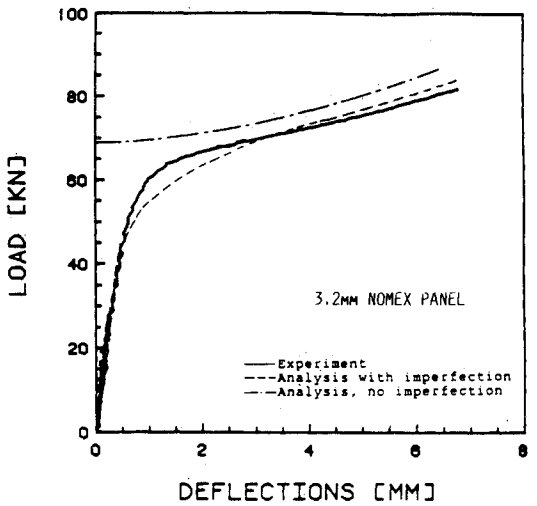

Fig. 10 Analytical and experimental deflections for 3.2-mm Nomex core panel.

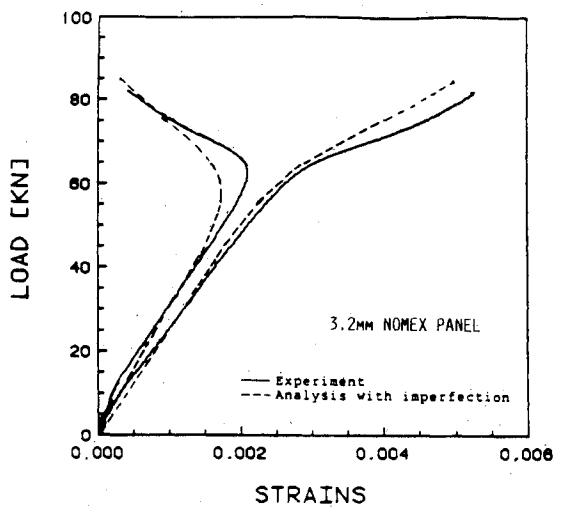

Fig. 11 Analytical and experimental strains for 3.2-mm Nomex core panel.

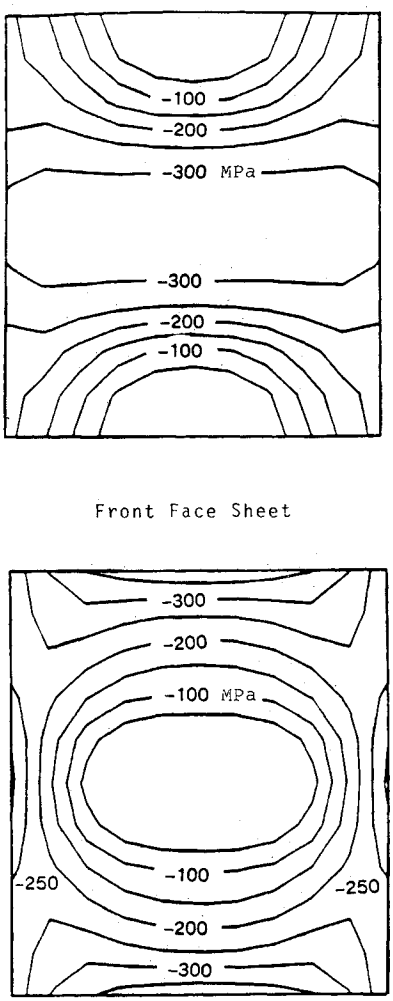

Fig. 12 Analytical σ_x stress contours on front and back faces of 3.2-mm Nomex core panel at load of 80 kN.

load-center deflection plots for one specimen of each family. As expected, the plate with an aluminum honeycomb core gave the highest loads for the 6.4-mm-thick cores. As will be shown later, the predicted buckling stress for these panels is slightly higher than the predicted face ultimate strength, but because of the initial imperfections present and the additional bending stresses caused thereof, those panels did not reach that predicted load. The Rohacell foam has the lowest shear modulus and therefore the lowest buckling loads. Additionally, its shear strength is the lowest of the three, as indicated in Table 1, so that the plates with a Rohacell core cannot go as far in the postbuckling range as the plate with a Nomex honeycomb core because failure always occurs in the core due to shear stresses. For the panel with a Nomex core, failure seems to have originated mostly at the bondline rather than in the honeycomb itself, since the Nomex honeycomb appears much stronger than the Rohacell foam. It seems also that manufacturer's value for the Nomex honeycomb shear strength are underestimated for the range of thicknesses used here.

Discussion

Comparison with Analytical Results

In order to interpret the experimental results, an anlysis technique was developed using a Reissner-Mindlin plate model to account for the transverse shear deformation in the core.[12-14] Geometric nonlinear terms and the effects of initial out-of-plane deflections were included in the analysis, since they were found to be of prime importance here. The Rayleigh-Ritz method was used to represent the plate deformation, and an efficient solution technique based on a direct minimizaiton of the potential energy was used to solve the nonlinear problem. Further details about this technique can be found in Ref. 8.

An example of the results obtained with the written computer code is shown in Figs. 10 and 11 for a plate with a 3.2-mm Nomex core. For these results, the magnitude of the initial imperfections included in the analysis were chosen so as to match the initial linear portion of the experimental load-deflection curve. As can be seen, the model used seems to represent the behavior of these sandwich plates quite well.

The other important information that can be obtained from this analysis is the stress fields in both the face sheets and in the core. For instance, the constant σ_x contours in the front and back face sheets are shown in Fig. 12. These were calculated for the same plate with a 3.2-mm Nomex core at approximately its experimental failure load of 80 KN, corresponding to an average stress of 190 MPa. Since the bending moments are of opposite signs at the center and at the clamped edges, the magnitude of the stresses is greatly increased at the center of the front face and at the loaded edge on the back face. The most important stresses acting on the core are the transverse shear stresses τ_{xz} and τ_{yz} shown in Fig. 13 for the same panel. The maximum value for τ_{xz} occurs

along the vertical centerline about halfway between the center of the plate and the clamped edges, while τ_{yz} occurs mainly in the corners and along the lateral sides. It is interesting to note that these stress distributions are qualitatively identical for all panels and that the predicted location of the maximum stresses, both in the faces and in the core, agrees well with the location where failure originated in the experiments.

Figure 14 shows the development of the maximum values for the stresses σ_x and τ_{xz} with increasing loading for the plates with 3.2- and 9.6-mm Nomex cores. These well illustrate the difference in behavior between thin and thick plates. The first point to notice is the rapid increase in stresses that occur above buckling. For the plate with a 3.2-mm-thick core, the shear stresses are the limiting factor, while for the plate with a 9.6-mm-thick core, the shear stresses remain smaller, since its core is thicker and the face strength is the important factor. Note also that if the shear strength of the bondline and core had been greater, then face fracture would have caused failure for the plate with a 3.2-mm core, but since the curve for σ_x vs P is so steep, the increase in load-carrying capability would have been relatively small.

Failure Parameters

Several times in the previous sections, differences between thin and thick panels have been made. These are somewhat qualitative notions, and it would be interesting to quantify these. One useful parameter is the plate width to thickness ratio, but it does not contain information about stiffness or failure. Looking back at the ultimate strength of buckled metallic plates, there are some semiempirical relations for predicting a plate ultimate load. A popular one is known as von Karman's equation, which relates the failure stress to the buckling and yielding stresses[15]:

$$\frac{\sigma_f}{\sigma_y} = \sqrt{\frac{\sigma_{cr}}{\sigma_y}}$$

where σ_f is the failure stress, σ_y the yield stress, and σ_{cr} the buckling stress. For composite material plates, however, several different modes can cause final failure instead of yielding alone. Still, a similar concept can be used to nondimensionalize the results that were obtained here by using the face ultimate strength σ_u as a reference. Then the following parameter

$$r = \sqrt{\frac{\sigma_u}{\sigma_{cr}}}$$

can be introduced as a measure of the panel stiffness, since thick and stiff panels will have a higher buckling load compared to the face ultimate than thin or soft ones. The experimental data are represented using this concept in Fig. 15, together with the curve for the von Karman's formula as reference (which, obviously, must be truncated at $\sigma_f = \sigma_u$). As one can see, the obtained points tend to concentrate in a definite region. Three reasons can explain why they do not reach the curve for the von Karman's equation:

1) The formula for metallic panels implicitly contains the beneficial effect of yielding. Strong stress concentrations arise in small regions of a buckled panel, and yielding can redistribute the load toward other regions so that the plate can go much further into the postbuckling range. In a composite material panel, there is little yielding and these stress concentrations lead more rapidly to failure.

2) Initial imperfections can reduce the failure load and are not included in the formula.

3) Other failure modes, e.g., core failure, can limit the postbuckling behavior.

Even with these limitations, this kind of plot allows one to get at least an estimate of the failure load based on the

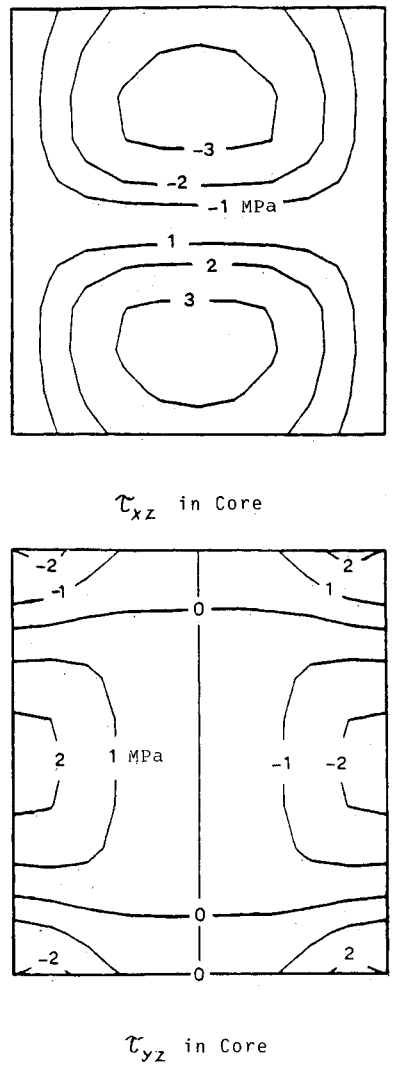

Fig. 13 Analytical τ_{xz} τ_{yz} stress contours in core of 3.2-mm Nomex core panel at load of 80 kN.

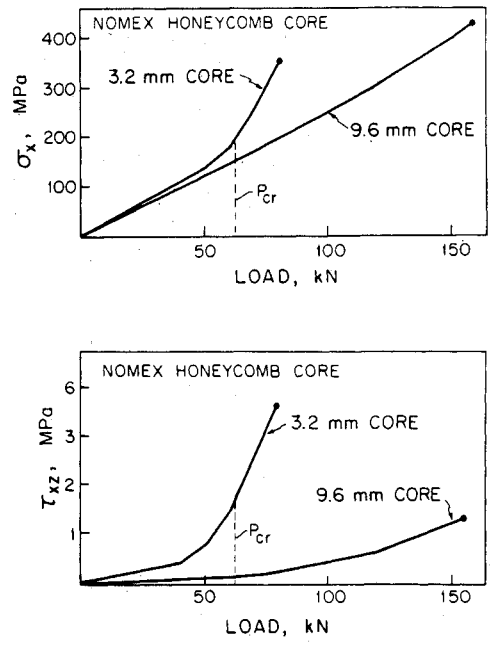

Fig. 14 Analytical maximum stresses σ_x and τ_{xz} for Nomex core panels.

Table 4 Predicted and experimental loads at buckling and final failure

Panel type		Analysis			Experiment		
Core type	Core thickness, mm	P Critical	P Failure		P Critical	P Failure	Observed failure mode
			Face	Core/bond			
Aluminum honeycomb	6.4	190	172	195	a	142	Face
Nomex honeycomb	3.2	68	91	81	62	82	Bond
Nomex honeycomb	6.4	123	133	127	116	128	Bond/face
Nomex honeycomb	9.6	178	169	184	a	152	Face
Rohacell	3.2	55	85	59	54	61	Core
Rohacell	6.4	81	121	91	90	94	Core
Rohacell	9.6	112	144	117	a	115	Core/face

All face sheets are $[+45/-45/0]_s$ graphite-epoxy. All loads in kN. [a]Buckling did not occur before failure.

buckling and ultimate stresses. It is also interesting to note that all the panels for which r was greater than approximately 1.3 failed in transverse shear, while for smaller values, face fracture was dominant.

Failure Prediction

Using the nonlinear analysis mentioned previously,[8] more accurate panel failure load predictions can be made. The first failure mode to examine is the core or bondline strength, and to do this, the maximum transverse shear stress criterion was used. For the Rohacell foam core, the manufacturer's value for the shear strength is 1.3 MPa, but for the Nomex panels, since no data was available on the bond strength, the inverse approach was used: taking on the P-w curve, the theoretical point closest to the actual failure point, the value of the maximum shear stress was found to be approximately 3.5 MPa for a plate with a 3.2 mm core and 3.7 MPa for a plate with a 6.4 mm core. The closeness of the two figures seems to support the fact that they are a reasonable estimate of the average bond strength. It is interesting to notice that the actual location of core fracture in the experiments is consistent with the location of the maximum shear stresses, as shown in Fig. 13.

The face fracture problem is more difficult, especially in compression and in the presence of multiaxial loading. This is also complicated by the fact that several different regions have potentially critical stresses, in particular the clamped edges and the center. To obtain a first approximation, a stress interaction failure criterion (Tsai-Wu-type) was used in a ply-by-ply analysis:

$$\left(\frac{1}{X_t}-\frac{1}{X_c}\right)\sigma_1+\left(\frac{1}{Y_t}-\frac{1}{Y_c}\right)\sigma_2+\frac{\sigma_1^2}{X_tX_c}+\frac{\sigma_2^2}{Y_tY_c}+\frac{\sigma_6^2}{S^2}=1$$

where σ_1, σ_2, and σ_6 are the ply stresses in ply axes, X_t and X_c the tensile and compressive ultimate parallel to fibers, Y_t and Y_c the transverse tensile and compressive ultimate, and S the shear ultimate.

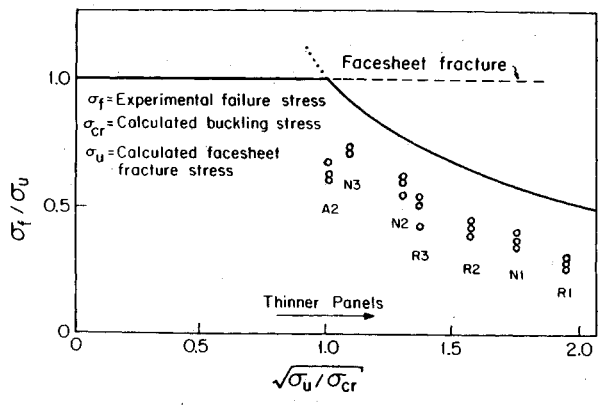

Fig. 15 Interaction between failure, buckling, and face ultimate stresses.

The predicted ultimate loads from the face and core criteria are shown in Table 4. In the same table, the experimental buckling loads are also indicated. The results are fairly good for the shear failure in the Rohacell core panels. For the face fracture, predictions are a little higher than the actual values, but this could be because the loading was never perfectly uniform in the tests, thus creating higher stresses along one side of the plates. The predicted most critical plies are always the 0-deg ones, due to their high stiffness and low strain to failure compared to the ± 45 deg set of plies. The most critical location is at the middle of the clamped edges, as is clearly visible in Fig. 12.

Conclusion

The core material properties and thickness have been shown to have a major influence on the behavior of sandwich panels under compression. For the range of values tested, only overall buckling occurred. Thin panels were observed to buckle into a regular first mode, but thick panels with soft core were observed to buckle into combination of first and second mode. Three types of failure modes were observed, core failure or bond failure for the thinner panels and face fracture for the thicker ones. Initial out-of-plane imperfections can also have an important influence on the final failure load for thick panels that cannot go very far into the postbuckling region, but only a small influence for thin panels. Using a nonlinear analysis, including the effect of transverse shear deformation and of initial out-of-plane imperfections, the behavior of sandwich panels can be well represented. Using the stresses predicted by this analysis and failure criteria for the appropriate failure mode, i.e., maximum transverse shear stresses for the core or bond failure and stress interaction for the face fracture, predictions of plate ultimate load can be made that are in good agreement with experimental data. Further work in this area should concentrate on testing a wider range of material properties and dimensions in order to observe other types of instabilities and failure modes. Also, the damage tolerance of sandwich structures and the influence of impact damage on the buckling behavior of sandwich panels needs to be investigated.

Acknowledgements

This work was supported by a joint Federal Aviation Administration/Navy program under contract N000019-85-C-0090.

References

[1]*Structural Sandwich Composites,* MIL-HDBK-23, U.S. Department of Defense, Washington, DC, 1968.

[2]Rao, K.M., "Buckling Analysis of Anisotropic Sandwich Plates Faced with Fiber-Reinforced Plastics," *AIAA Journal,* Vol. 23, Aug. 1985, pp. 1247-1253.

[3]Benson, A.S. and Mayers, J., "General Instability and Face Wrinkling of Sandwich Plates: Unified Theory and Applications," *AIAA Journal,* Vol. 5, April 1967, pp. 729-739.

[4]Arnolds, R.R. and Mayers, J., "Buckling, Postbuckling and Crippling of Materially Nonlinear Laminated Composite Plates," *International Journal of Solids and Structures,* Vol. 20, 1984, pp. 863-880.

[5]Kuenzi, E.W., Norris C.B., and Jenkinson, P.M., "Buckling Coefficients for Simply-Supported and Clamped Sandwich Panels under Edgewise Compression," Forest Product Laboratory, U.S. Department of Agriculture, Note FPL070, 1964.

[6]Leissa, A.W., "Buckling of Laminated Composite Plates and Shell Panels," Air Force Wright Aeronautical Laboratories, AFWAL-TR-85-3069, June 1985.

[7]Pearce, T.R.A. and Webber, J.P.H., "Experimental Buckling Loads of Sandwich Panels with Carbon Fiber Face Plates," *Aeronautical Quarterly,* Vol. 24, Nov. 1973, pp. 295-312.

[8]Minguet, P.J., "Buckling of Graphite/Epoxy Sandwich Plates," M.S. Thesis, Dept. of Aeronautics and Astronautics, Massachusetts Insititue of Technology, Cambridge, May 1986. Also TELAC R. 86-16, M.I.T., May 1986.

[9]Vizzini, A.J. and Lagace, P.A., "The Role of Ply Buckling in the Compressive Failure of Graphite/Epoxy Tubes," *AIAA Journal,* Vol. 23, Nov. 1985, pp. 1791-1797.

[10]Lagace, P.A. and Brewer J.C., *TELAC Manufacturing Class Notes,* unpublished, 1981.

[11]Jensen, D.W., "Buckling and Postbuckling Behavior of Unbalanced and Unsymmetric Laminated Graphite/Epoxy Plates," Ph.D. Thesis, Dept. of Aeronautics and Astronautics, Massachusetts Institute of Technology, Jan. 1986. Also, TELAC Rept. 86-3, M.I.T., Jan. 1986.

[12]Mindlin, R.D., "Influence of Rotatory Inertia and Shear on Flexural Motion of Isotropic Elastic Plates," *Journal of Applied Mechanics,* Vol. 18, March 1951, pp. 31-38.

[13]Reissner, E., "The Effect of Transverse Shear Deformation on the Bending of Elastic Plates,"*Journal of Applied Mechanics,* Vol. 12, June 1945, pp. A69-A77.

[14]Whitney, J.M., "Stress Analysis of Thick Laminated Composite and Sandwich Plates," *Journal of Composite Materials,* Vol. 6, Oct. 1972, pp. 426-440.

[15]Timoshenko, S.P. and Gere, J.M., *Theory of Elastic Stability,* 2nd ed., McGraw-Hill, New York, 1961.